# A Practical Integrated Fault Location Technique for Radial Power Distribution Systems

HAMDOUCHE Tarek
Dept. Process Automation and Electrification
Electrification Laboratory of Industrial Enterprises (LREEI)
University of Boumerdes
Boumerdes, Algeria
t.hamdouche@univ-boumerdes.dz

BENDJEGHABA Omar
Dept. Process Automation and Electrification
Electrification Laboratory of Industrial Enterprises (LREEI)
University of Boumerdes
Boumerdes, Algeria
bendjeghaba@univ-boumerdes.dz

AHRICHE Aimed
Dept. Electrical Engineering
University of Boumerdes
Boumerdes, Algeria
a.ahriche@univ-boumerdes.dz

***Abstract*— power distribution systems (PDS) are becoming more complex and dispersed at long distances and different locations. With its radial and several laterals configuration, loads could be connected at similar distances from the substation which leads to a multi estimation of fault location and consuming more time for iterative fault location algorithms. In order to overcome those difficulties, a practical integrated fault location method for radial PDS is presented in this paper. The basic idea of the proposed approach is to partition a multi lateral distribution system to possible mono lateral system (MLSs) by a proposed communicant sensor (CS). Then an impedance based algorithm is applied only at the faulty MLS. To examine the whole method in the field, a real PDS from the Algerian distribution grid is used. Experimental results present significant benefits compared to a previous method reported in the literature.**

***Keywords*—Power distribution systems; fault location; service continuity ;comminicant sensors.**

## I. INTRODUCTION

Service continuity and power quality are great challenges for power distribution companies, and it is also a very important condition needed by customers and investors. Outage time caused by faults is considered as a paid and not supplied power which is a failure for distribution companies. Due to the increasing demand on electric power, electric grid becomes more extended and more complex, which make it subject to faults caused by different events, such as atmospheric factors, equipments degradation, transport accidents, etc. In order to improve the operation indexes such as SAIDI (System Average Interruption Duration Index) and CAIDI (Customers Average Interruption Duration Index), faults location must be done very fast. This objective is quite mature in transmission power systems (TPS) where lines are homogeneous and have a simple topology. On the other hand, in distribution power systems (DPS), fault location task is very complex because of some inherent characteristics such as; radial architecture, laterals and sub laterals, different kinds and sections of cables, dynamic topology, unbalanced operation, time varying load and fault resistance. All of these make PDS a heterogeneous system. Until now, when a fault occurs in the PDS, a maintenance crew is sent to patrol the feeder, guided by fault indicator (FI) devices installed at different line-sections. Often, these devices are not operational and needing a regular maintenance. Another method is the dividing of the feeder into isolate sub regions using breaker recloser and sensors of SCADA (Supervisory Control And Data Acquisition). This method is practical and efficient, but it is not suitable for feeder equipments. It caused damages when reclose on the short circuit current. Owing to the cost and time consuming, these methods may not be an economical solutions. Hence, automatic fault location is an essential issue to speed up the restoration system and improve the operation indexes for distribution companies. Before, several efficient techniques have been proposed for fault location in PDS. They can be classified into three main families; travel wave based methods [1-3], artificial intelligent based methods [4-11], impedance based methods [12-15]. The first category is based on the high frequencies signals generated by faults and traveling along the feeder. These methods are fast and show a high accuracy. However they require high sampling rate for digital relays and high number of sensors due to the huge number of laterals and ramifications in PDS. In addition, in case of high resistive faults the generated wave is weak and can be fully dissipated which affect the efficiency of travel wave methods. In the second category, a machine learning rule is used to interpret the complex relationship between the fault and its distance from the source. Different artificial intelligent techniques are used such as; Fuzzy Logic (FL) [4], [5]. Artificial Neural Networks (ANN) [6], [7], Supporting Vector Regression (SVR) [8], [9], Genetic Algorithms (GA) [10], [11]. Providing an adequate and sufficient dataset is the common condition of those techniques. For example in work [7] a fault location technique for radial distributions networks is proposed. In this method short circuit power peaks are measured at the main substation during faulty conditions at different distances from the source. The method presents a good accuracy, but it is not a generalized one. Because two phase to ground (LLG) and tree phase to ground (LLLG) faults are not considered. In addition, loads variations are supposed

978-1-7281-2220-5/19/$31.00 ©2019 IEEE

fixed in the time, which need to update the gathering dataset at any change of the feeder topology, and leading to time consuming at the ANN learning step. The third category is the impedance based methods, when fault voltages and currents seen at the beginning of the feeder are used to calculate the apparent impedance. Because of their simplicity and low implementation cost, they are the most used one. However, owing to multi branches, loads uncertainty and faults resistances multi estimation location is the main drawback of these methods. Generally, impedance based algorithms used iterative estimations which may converge at false solution. In reference [13], an iterative fault location algorithm is proposed. The algorithm use a load current estimation model base on the assumption that, impedance load is constant and known, which it's not always true and available in PDS. So, the fault distance can be out of the section and the algorithm would be executed for the next section, leading to more time consuming. Paper [14] presents a novel fault location method. By traversing all value of fault distance the algorithm overcomes the problem of false solution for iterative methods. A high accuracy has obtained, but the effect of load uncertainty is not treated. In work [15], an iterative approach is presented considering load variations by aggregating the total load at the end of the feeder. An initial fault distance at each line section is assumed and incremented from zero to the section length. Then the fault location is obtained were the fault reactance is minimum. The method shows a good performance, but it requires a high number of tests. On the other hand, this algorithm neglects the problem of multiple estimation location, which is the main pitfall of all impedance based methods. In order to overcome this problem, a practical integrated fault location technique is proposed in this paper. By knowing the topology of the feeder, it can be segmented into a number of mono lateral systems (MLSs) using a proposed communicant sensor (CS), which is judicially installed in radial PDS. Then, a fault location process is applied only at the affected MLS basing on an equivalent model of the feeder. The proposed method can help impedance based algorithms by reducing the number of iterations and giving a unique fault location. The rest of the paper is organized as follows; section II describes the proposed fault location approach. Next, in section III tests and analysis of the proposed method on the IEEE 13 Node test feeder and a real PDS is presented. Then, section IV is reserved for the conclusion.

## II. PROPSED FAULT LOCATION METHOD

The proposed fault location method integrates apparent impedance calculation using voltages and currents seen from the beginning of the feeder with transmitted information of a proposed CS to determine possible fault location. The basic idea of the technique is to segment a multi laterals distribution system to possible MLSs by CSs. The number and placement of the used CSs is depending on the feeder topology, which assumed to be known. The method bases on two steps. Firstly, a transmitted fault signal is generated from the CS to the dispatching station. So, the faulty MLS is precisely detected. Then, in the second step an impedance based algorithm is applied only at the faulty MLS using an established equivalent model for the feeder during faulty conditions. Details of each step are described in the following sections.

### *A. The Proposed Communicant sensor*

Due to the development and evolution of telecommunication supports and infrastructures in recent years, most of geographical areas are covered by telecommunication network. The idea of the sensor presented in this work is to interpret the detected fault current to a communication signal using a proposed circuit, as illustrated in Fig. 1.

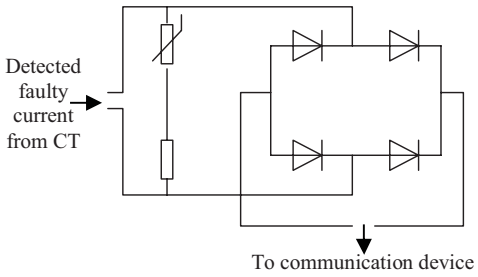


Fig.1. Connexion circuit

### *B. Fault location estimation using impedance based method*

The proposed impedance methodology is based on the minimum fault reactance concept [15-17]; a fault reactance is calculated for each assumed distance, this procedure is repeated to cover the entire feeder length. Considering the resistive nature of faults, the estimated fault location is the distance where the fault reactance is smaller. The fact that voltages and currents measurements are often available only at the beginning of the feeder, it is difficult to obtain the online impedance at each node. In order to consider the load variations, several impedance based algorithms proceeding to aggregate the total load at the farthest node of the feeder [15]. This strategy is adopted in this study, basing on the assumption that the aggregated load impedance $Z_c$ [3x3] is bigger than line impedance $Z_l$ [3x3]. From Fig. 2, we can get:

$$Z_c = (V_s / I_s) - Z_l \quad (1)$$

Where $V_s$ [3x1] and $I_s$ [3x1] are the sending-end pre-fault voltages and currents, respectively. $Z_l = \Sigma Z_{LMLSj}$, $j$ is varied from 1 to total *MLSs* number $n$; with $\Sigma Z_{LMLSj}$ [3x3] is the series impedance of each homogeneous line sections.

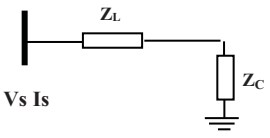


Fig. 2. Simplified single line
feeder model during prefault conditions

One of difficulties of the technique proposed in [15] is the multiple fault location estimation caused by feeder laterals. In the here presented methodology, by detecting the exact faulty *MLS* the other healthy *MLSs* can be eliminated from the fault location process which leads to reduce the number of analyzed line sections and giving a unique fault location estimation.

During a fault, the equivalent model of the feeder is presented as shown in Fig. 3.

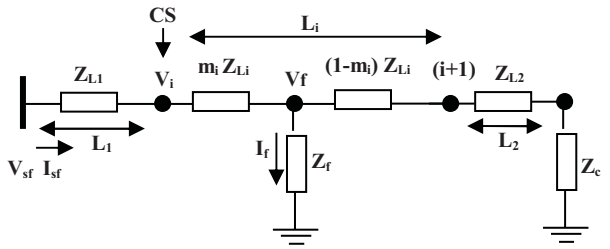


Fig. 3. Equivalent model of the feeder during faulty conditions

Where:
$L_1$: The distance from the substation to the faulted *MLS*.
$L_2$: The distance from the faulted *MLS* to the end of the feeder.
$i$: the faulty *MLS*.
$L_i$: The faulty *MLS* length.
$Z_{Li}$ [3x3]: the faulty *MLS* impedance.
$Z_{L1}$ [3x3] = $\Sigma\, Z_{LMLSj}$, $j$ is varied from 1 to ($i$-1).
$Z_{L2}$ [3x3] = $\Sigma\, Z_{LMLSj}$, $j$ is varied from ($i$+1) to n.
$V_{sf}$ [3x1]: voltage at the substation during the fault.
$I_{sf}$ [3x1]: current at the substation during the fault.
$m_i$: the per unit fault distance at $MLS_i$.

From Fig. 3 the fault location $L_f$ is determined using (2).

$$L_f = L_1 + m_i L_i \tag{2}$$

The incoming voltages $V_i$ [3x3] at node ($i$), voltages at fault point $V_f$ [3x3], and fault currents $I_f$ [3x3] are obtained using (3), (4) and (5) respectively.

$$V_i = V_{sf} - Z_{L1} I_{sf} \tag{3}$$

$$V_f = V_i - m_i Z_{li} I_{sf} \tag{4}$$

$$I_f = (I_{sf}) - (((1 - m_i) Z_{Li} + Z_{L2} + Z_c)^{-1} V_s) \tag{5}$$

Then the fault impedance is;

$$Z_F(m_i) = (V_f(m_i) / I_f(m_i)) \tag{6}$$

$$X_F(m_i) = imag\,(Z_F(m_i)) \tag{7}$$

Basing on the resistive character of faults, and by incrementing the assumed distance ($m_i$) from zero to 1, the fault location is assumed at the distance where the fault reactance is minimal. The flow chart of the proposed method is depicted in Fig. 4.

## III. TESTS AND ANALYSIS

The IEEE 13 Node test feeder is selected in this study, in order to validate the performance of the proposed fault location method. For more details of this test feeder, readers can refer to [18]. A modified model of the test feeder is simulated using the Simulink toolbox of MATLAB environment [19]. A phase to ground fault is simulated at different locations throughout the feeder and used to verify the accuracy of the method (F1 at Node 684, F2 at node 675, and F3 at node 680). The segmentation of the IEEE 13 Node feeder to possible MLSs is assumed as shown in Fig. 5.

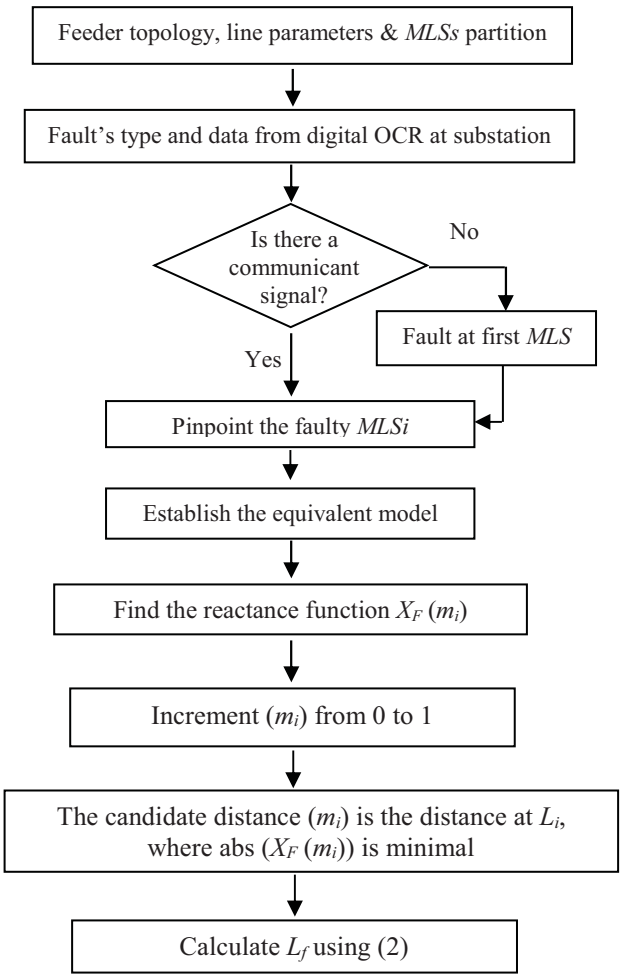


Fig. 4. Flow chart of the proposed method

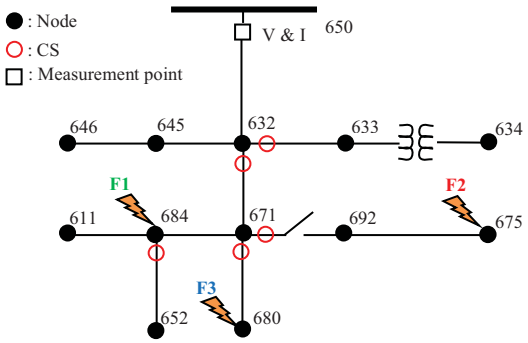


Fig. 5. Possile MLS's partition for the modified IEEE 13 Node feeder.

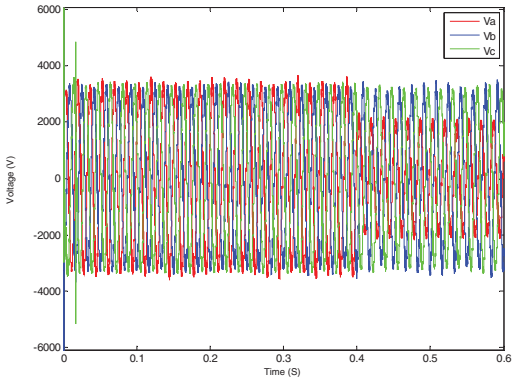


Fig. 6. F1 volatges at substation from the IEEE 13 Node test feeder

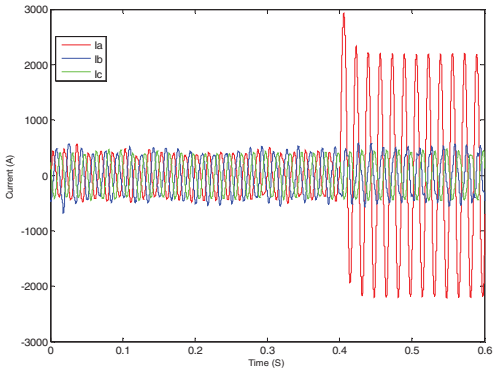


Fig. 7. F1 currents at substation from the IEEE 13 Node test feeder.

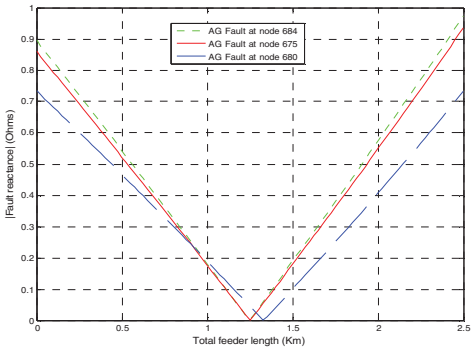


Fig. 8. Faults reactance (absolute values) in the IEEE 13 Node feeder using method of reference [15]

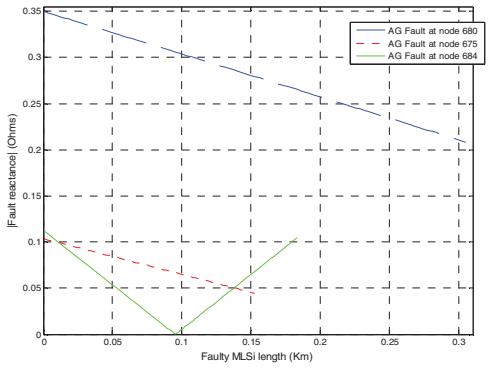


Fig. 9. Faults reactance (absolute values) in the IEEE 13 Node feeder using the proposed method.

Fig. 6 and Fig. 7, show the three phase voltages and currents measered at the beginning of the feeder before and during the fault (F1). The fundamental components are calculated using fourier transform and used as data input. From Fig. 8, the results show that the application of the method presented in [15] presents a considerable accuracy. however, the number of candidates fault location estimation is strongly depended on the number of feeder's branchs. From Fig. 9, results show a benefit accuracy by using the here proposed method. The healty MLSs impedances $Z_{L1}$, $Z_{L2}$ are identified. Then, the fault location process excuted only at the faulty *MLSi*, which reduce the number of iteration tests and giving a unique fault location estimation. The errors are calculated by (8), and recapitulated in table I.

$$Error(\%) = (|\, l_{real} - l_{est} \,|/\, l_t\,) \times 100 \qquad (8)$$

Where $l_{real}$ is the real length from the mesurement point to the fault, $l_{est}$ is the estimated fault, and $l_t$ is the total length of the feeder.

TABLE I. RESULTS COMPARAISON (IEEE 13 NODE TEST FEEDER)

| **Faults type** | **Proposed method using approach 1 error (%)** | **Method [15] error (%)** | **Candidates fault location estimation** | |
|---|---|---|---|---|
| | | | ***Proposed method*** | ***Method [15]*** |
| F1 | 0,146 | 2,426 | 1 | 2 |
| F2 | 0,000 | 4,865 | 1 | 2 |
| F3 | 0,000 | 7,962 | 1 | 2 |

To examine the method in the field, a real PDS from the Algerian distribution grid is used; its topology is presented in Fig. 9. The selected system is 51 nodes, 30 KA underground feeder, dispersed at a total length of 18,357 Km with a total power of 15,933 MVA. The additional information of this feeder is shown in Table III in Appendix. From the topology of the feeder, it can be divided into four MLSs. Thus, three CSs are needed to be installed, as shown in Fig. 9.

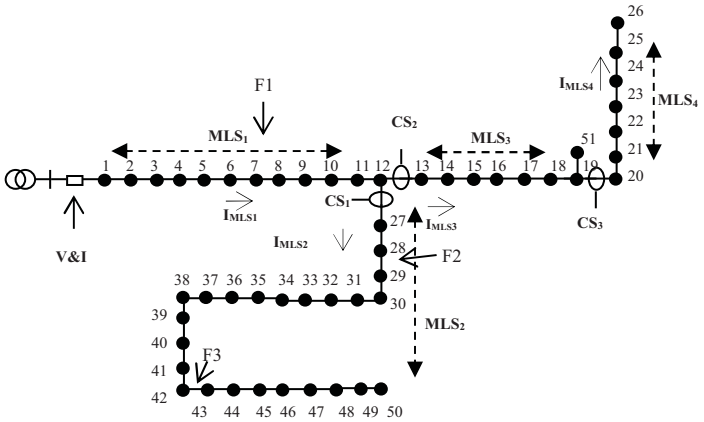


Fig. 9. Test feeder topology from the Algerian distribution grid

To evaluate the performance of the proposed method, three real single phase to earth faults cases are used. Those faults are happened at different load conditions and different locations along the feeder length. F1 (at 3220 m), F2 (5927 m), and F3 (at 10290 m). Fig. 10 presents voltages and currents measured at the beginning of the feeder for a single line to ground fault, extracted from the digital OCR at the substation.

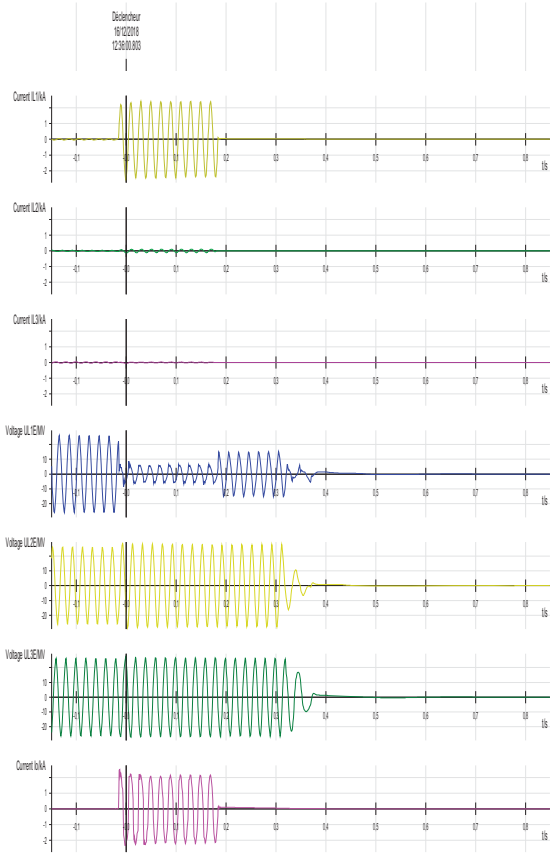

Fig. 10. Currents and voltages recorded at the substation during a single phase to ground fault.

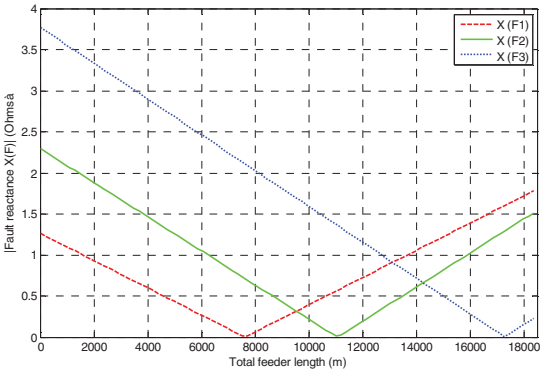


Fig. 11. Faults reactance (absolute values) using method of reference [15]

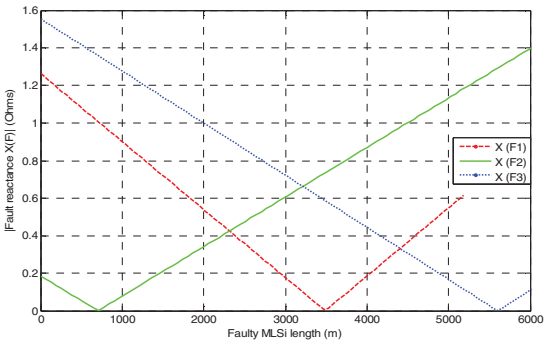


Fig. 12. Faults reactance (absolute values) using the proposed method.

The experemental results shown in Fig. 11 and Fig. 12, confirm the perfermance of the proposed method by giving a high accuracy at different fault locations under different load conditions and giving a unique fault location compared to the privious method. Errors etstimations are calculated using (8), and presented in table II.

TABLE II. RESULTS COMPARISONS (ALGERIAN GRID FEEDER)

| **Faults** | **Proposed method using approach1 error (%)** | **Method [15] error (%)** | **Candidates fault location estimation** | |
|---|---|---|---|---|
| | | | ***Proposed method*** | ***Method [15]*** |
| F1 | 2,879 | 6,460 | 1 | 1 |
| F2 | 0,855 | 3,715 | 1 | 2 |
| F3 | 0,119 | 0,054 | 1 | 2 |

The experimental environment for testing the proposed sensor is shown in Fig. 13. The CS is calibrated according to the over current relay (OCR) threshold in order to satisfy the coordination.

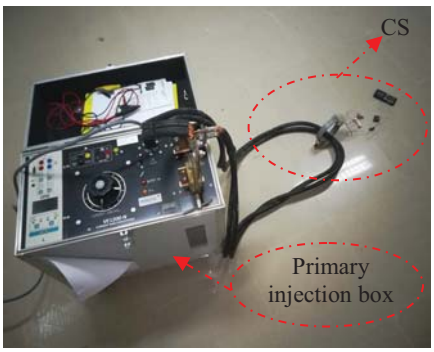


Fig. 13. Experimental environment for testing and calibrating the Proposed CS

## III. CONCLUSION

A practical integrated technique to locate faults in radial distribution systems is exposed in this paper. This method overcomes the problem of multi fault location estimations, which is the main drawback of impedance based algorithms. By segmenting the PDS to possible MLSs, the fault location process executed only at a partition of the system and giving

unique fault location estimation, which leading to speed up the fault location process. The method requires only information of feeder topology, series line impedance of each homogeneous section, voltages and currents fundamental components measured at substation pre and during faulty conditions. The simulation and experimental results demonstrate the accuracy improvements and feasibility of the proposed method.

## REFERENCES


[1] H. Fernando Magnago, A. Aburn, "A New Fault Location Technique for Radial Distribution Systems Based on High Frequency Signals," IEEE Power Engineering Society Summer Meeting. Conference Proceedings (Cat. No.99CH36364), vol.1, pp. 421-431, 1999.

[2] M. Goudarzi, B.Vahidi, R.A. Naghizadeh, S.H. Hosseinian, "Improved fault location algorithm for radial distribution systems with discrete and continuous wavelet analysis," Electrical Power and Energy Systems 67 (2015) 423-430.

[3] A. Ghaderi, H. Ali Mohammadpour, H. Giin "Active Fault Location in Distribution Network using Time-Frequency Reflectometry," IEEE Power and Energy Conference at Illinois (PECI), pp. 1-7, 2015.

[4] J. Moshtagh, A. Rafinia, "A New Approach to High Impedance Fault Location in Three-Phase Underground Distribution System Using Combination of Fuzzy Logic & Wavelet Analysis," 11th International Conference on Environment and Electrical Engineering, pp. 90-97, 2012

[5] S. Bunjongjit, A. Ngaopitakkul, C. Pothisarn "A Discrete Wavelet Transform and Fuzzy Logic Algorithm for Identifying the Location of Fault in Underground Distribution System," International Conference on Fuzzy Theory and Its Applications (iFUZZY), pp. 415-419, 2013.

[6] H. Zayandehroodi, A. Mohamed, M. Farhoodnea and A. Heidari "New Training Strategies for RBF Neural Networks to Determine Fault Location in a Distribution Network with DG Units," IEEE 7th nternational Power Engineering and Optimization Conference (PEOCO), pp. 450-454, 2013.

[7] P. Farzan, M. Izadi, C. Gomes, and M. Zainal"Short Circuit Power Based Fault Location Algorithm in Distribution Networks," IEEE 8th International Power Engineering and Optimization Conference (PEOCO2014), pp. 105-109, 2014.

[8] L. Ye, D. You, X. Yein, K. Wang, and J. Wu "An improved fault location method for distribution system using wavelets and support vector regression," Electrical Power and Energy Systems 55 (2014) 467-472.

[9] S. Shilpa, H. Mokhlis, H. Azil, A. Abu bakar, and L. Awalin "Fault Location in an Unbalanced Distribution System using Support Vector Classification and Regression Analysis," IEEJ Transactions on Electrical and Electronic Engeneering. 2018; 13: 237–245.

[10] S. Jamali, A. Bahmanyar, and H. Borhani-Bahabadi "A Fast and Accurate Fault Location Method for Distribution Networks with DG Using Genetic Algorithms," Smart Grid Conference (SGC), pp. 110-114, 2015.

[11] J. Qiyan, J. Rong "Fault Location for Distribution Network Based on Genetic Algorithm and Stage Treatment," Spring Congress on Engineering and Technology, pp. 1-4, 2012

[12] IEEE Guide for Determining Fault Location on AC Transmission and Distribution Lines, pp. 1-76, 2015.

[13] S. Lee, M. Choi, S. Kang, B. Jin, D. lee, B. Ahn, N. Yoon, H. Kim, and S. Wee. "An Intelligent and Efficient Fault Location and Diagnosis Scheme for Radial Distribution Systems," IEEE Transactions on power delivery, vol. 19, NO. 2, April 2004.

[14] Y. Lei, Y. Dahai, Y. Xianggen, T. Jinrui, L. Baolei, and Y. Yuan, " A Novel Fault-Location Method for Radial Distribution Systems," Asia pacific power and energy engineering conference, pp. 1-5, 2012.

[15] G. Espana, M. Florez, and V. Tores, "Fault location method based on the determination of the minimum fault reactance for uncertainty loaded and unbalanced power distribution systems," IEEE/PES Transmission and Distribution conference and exposition; Latina America, pp. 803-809, 2010.

[16] A. Hoke, R. Butler, J. Hambrick, B. Kroposki, " Steady state analysis of maximum photovoltaic penetration levels on typical distribution feeders" IEEE Transsustain Energy 2013; 4:350-7.

[17] C. Orozco-Henao, A. S. Bretas, R. Chouhy-Leborgne, A. R. Herrera, J. Marin-Quintero, " Active distribution network fault location methodology: A minumum fault reactance and Fibonacci search approach" Electic Power and Energy Systems 84 (2017) 232-241.

[18] W. H. Kersting, "Radial distribution test feeders," IEEE Power Engeniring Society winter meeting, 2001.

[19] Mathworks Matlab. Natick, MA, 2012. [Online]. Available: http:// www.mathworks.com/..


## APPENDIX

TABLE III. FIELD FEEDER CHARACTERISTICS

| From | To | Conductor type | Sec (mm2) | Long (Km) | R (Ω/Km) | X (Ω/Km) | St (Kva) | Accumulated distance (m) |
|---|---|---|---|---|---|---|---|---|
| 1 | 2 | AA | 120,000 | 1,021 | 0,255 | 0,102 | 0,00 | 1021 |
| 1 | 2 | AA | 120,000 | 0,318 | 0,080 | 0,032 | 0,00 | 1339 |
| 1 | 2 | CU | 70,000 | 0,418 | 0,107 | 0,042 | 250,00 | 1757 |
| 2 | 3 | CU | 70,000 | 0,138 | 0,035 | 0,014 | 0,00 | 1895 |
| 2 | 3 | AA | 120,000 | 0,019 | 0,005 | 0,002 | 250,00 | 1914 |
| 3 | 4 | AA | 120,000 | 0,019 | 0,005 | 0,002 | 0,00 | 1933 |
| 3 | 4 | CU | 70,000 | 0,033 | 0,008 | 0,003 | 400,00 | 1966 |
| 4 | 5 | CU | 70,000 | 0,067 | 0,017 | 0,007 | 250,00 | 2033 |
| 5 | 6 | CU | 70,000 | 0,052 | 0,013 | 0,005 | 0,00 | 2085 |
| 5 | 6 | AA | 120,000 | 0,170 | 0,043 | 0,017 | 400,00 | 2255 |
| 6 | 7 | AA | 120,000 | 0,170 | 0,043 | 0,017 | 0,00 | 2425 |
| 6 | 7 | CU | 70,000 | 0,196 | 0,050 | 0,020 | 630,00 | 2621 |
| 7 | 8 | AA | 120,000 | 0,127 | 0,032 | 0,013 | 400,00 | 2748 |
| 8 | 9 | AA | 120,000 | 0,072 | 0,018 | 0,007 | 160,00 | 2820 |
| 9 | 10 | CU | 120,000 | 0,040 | 0,006 | 0,004 | 0,00 | 2860 |
| 9 | 10 | AA | 120,000 | 0,150 | 0,038 | 0,015 | 0,00 | 3010 |
| 9 | 10 | AA | 120,000 | 0,459 | 0,115 | 0,046 | 400,00 | 3469 |
| 10 | 11 | AA | 120,000 | 0,481 | 0,120 | 0,048 | 250,00 | 3950 |
| 11 | 12 | AA | 120,000 | 0,119 | 0,030 | 0,012 | 400,00 | 4069 |
| 12 | 13 | AA | 120,000 | 0,310 | 0,078 | 0,031 | 250,00 | 4379 |

| | | | | | | | | |
|---|---|---|---|---|---|---|---|---|
| 13 | 14 | AA | 120,000 | 0,805 | 0,201 | 0,081 | 400,00 | 5184 |
| 14 | 15 | AA | 120,000 | 0,597 | 0,149 | 0,060 | 250,00 | 5781 |
| 15 | 16 | AA | 120,000 | 0,518 | 0,130 | 0,052 | 250,00 | 6299 |
| 16 | 17 | AA | 120,000 | 0,315 | 0,079 | 0,032 | 250,00 | 6614 |
| 17 | 18 | AA | 120,000 | 0,203 | 0,051 | 0,020 | 250,00 | 6817 |
| 18 | 19 | AA | 120,000 | 0,515 | 0,129 | 0,052 | 250,00 | 7332 |
| 19 | 20 | AA | 120,000 | 1,247 | 0,312 | 0,125 | 400,00 | 8579 |
| 20 | 21 | AA | 120,000 | 0,029 | 0,007 | 0,003 | 0,00 | 8608 |
| 20 | 21 | CU | 120,000 | 0,340 | 0,051 | 0,034 | 400,00 | 8948 |
| 20 | 21 | AA | 120,000 | 0,695 | 0,174 | 0,070 | 160,00 | 9643 |
| 21 | 22 | AA | 120,000 | 0,586 | 0,147 | 0,059 | 250,00 | 10229 |
| 22 | 23 | AA | 120,000 | 0,338 | 0,085 | 0,034 | 400,00 | 10567 |
| 23 | 24 | AA | 120,000 | 0,426 | 0,107 | 0,043 | 250,00 | 10993 |
| 24 | 25 | AA | 120,000 | 0,586 | 0,147 | 0,059 | 250,00 | 11579 |
| 25 | 26 | AA | 120,000 | 0,343 | 0,086 | 0,034 | 250,00 | 11922 |
| 26 | 27 | AA | 120,000 | 0,490 | 0,123 | 0,049 | 410,00 | 12412 |
| 27 | 28 | AA | 120,000 | 0,103 | 0,026 | 0,010 | 160,00 | 12515 |
| 28 | 29 | AA | 120,000 | 0,492 | 0,123 | 0,049 | 0,00 | 13007 |
| 29 | 30 | CU | 70,000 | 0,190 | 0,049 | 0,019 | 0,00 | 13197 |
| 29 | 30 | CU | 120,000 | 0,143 | 0,021 | 0,014 | 100,00 | 13340 |
| 30 | 31 | CU | 120,000 | 0,194 | 0,029 | 0,019 | 0,00 | 13534 |
| 30 | 31 | AA | 120,000 | 0,033 | 0,008 | 0,003 | 630,00 | 13567 |
| 31 | 32 | AA | 120,000 | 0,033 | 0,008 | 0,003 | 0,00 | 13600 |
| 31 | 32 | CU | 120,000 | 0,138 | 0,021 | 0,014 | 250,00 | 13738 |
| 32 | 33 | AA | 120,000 | 0,159 | 0,040 | 0,016 | 630,00 | 13897 |
| 33 | 34 | AA | 120,000 | 0,114 | 0,029 | 0,011 | 0,00 | 14011 |
| 33 | 34 | CU | 120,000 | 0,058 | 0,009 | 0,006 | 0,00 | 14069 |
| 33 | 34 | CU | 120,000 | 0,023 | 0,003 | 0,002 | 630,00 | 14092 |
| 34 | 35 | CU | 120,000 | 0,020 | 0,003 | 0,002 | 0,00 | 14112 |
| 34 | 35 | CU | 120,000 | 0,239 | 0,036 | 0,024 | 160,00 | 14351 |
| 35 | 36 | CU | 70,000 | 0,248 | 0,064 | 0,025 | 630,00 | 14599 |
| 36 | 37 | CU | 70,000 | 0,210 | 0,054 | 0,021 | 463,00 | 14809 |
| 37 | 38 | AA | 120,000 | 0,346 | 0,087 | 0,035 | 0,00 | 15155 |
| 37 | 38 | AA | 120,000 | 0,119 | 0,030 | 0,012 | 0,00 | 15274 |
| 37 | 38 | AA | 120,000 | 0,190 | 0,048 | 0,019 | 250,00 | 15464 |
| 39 | 40 | AA | 120,000 | 0,229 | 0,057 | 0,023 | 0,00 | 15693 |
| 39 | 40 | AA | 120,000 | 0,037 | 0,009 | 0,004 | 400,00 | 15730 |
| 40 | 41 | AA | 120,000 | 0,042 | 0,011 | 0,004 | 400,00 | 15772 |
| 41 | 42 | CU | 70,000 | 0,231 | 0,059 | 0,023 | 0,00 | 16003 |
| 41 | 42 | CU | 70,000 | 0,046 | 0,012 | 0,005 | 0,00 | 16049 |
| 41 | 42 | AA | 120,000 | 0,148 | 0,037 | 0,015 | 400,00 | 16197 |
| 42 | 43 | AA | 120,000 | 0,142 | 0,036 | 0,014 | 0,00 | 16339 |
| 42 | 43 | CU | 120,000 | 0,086 | 0,013 | 0,009 | 0,00 | 16425 |
| 42 | 43 | CU | 70,000 | 0,058 | 0,015 | 0,006 | 250,00 | 16483 |
| 43 | 44 | AA | 120,000 | 0,245 | 0,061 | 0,025 | 400,00 | 16728 |
| 44 | 45 | AA | 120,000 | 0,240 | 0,060 | 0,024 | 0,00 | 16968 |
| 44 | 45 | AA | 120,000 | 0,035 | 0,009 | 0,004 | 250,00 | 17003 |
| 45 | 46 | AA | 120,000 | 0,034 | 0,009 | 0,003 | 0,00 | 17037 |
| 45 | 46 | CU | 70,000 | 0,185 | 0,048 | 0,019 | 160,00 | 17222 |
| 46 | 47 | CU | 70,000 | 0,032 | 0,008 | 0,003 | 0,00 | 17254 |
| 46 | 47 | CU | 120,000 | 0,070 | 0,011 | 0,007 | 0,00 | 17324 |
| 46 | 47 | AA | 120,000 | 0,142 | 0,036 | 0,014 | 160,00 | 17466 |
| 47 | 48 | AA | 120,000 | 0,148 | 0,037 | 0,015 | 160,00 | 17614 |
| 48 | 49 | CU | 120,000 | 0,070 | 0,011 | 0,007 | 0,00 | 17684 |
| 48 | 49 | CU | 70,000 | 0,170 | 0,044 | 0,017 | 0,00 | 17854 |
| 48 | 49 | CU | 70,000 | 0,163 | 0,042 | 0,016 | 0,00 | 18017 |
| 48 | 49 | CU | 120,000 | 0,030 | 0,005 | 0,003 | 400,00 | 18047 |
| 49 | 50 | CU | 120,000 | 0,030 | 0,005 | 0,003 | 0,00 | 18077 |
| 49 | 50 | CU | 70,000 | 0,060 | 0,015 | 0,006 | 0,00 | 18137 |
| 49 | 50 | CU | 120,000 | 0,110 | 0,017 | 0,011 | 250,00 | 18247 |
| 50 | 51 | CU | 120,000 | 0,110 | 0,017 | 0,011 | 400,00 | 18357 |